Deep Learning for The Detection of COVID-19 Using Transfer Learning and Model Integration

Ningwei Wang, Hongzhe Liu*, Cheng Xu
Beijing Key Laboratory of Information Service Engineering
Beijing Union University
Beijing, 100101, China 191083510919@buu.edu.cn

Abstract—**We researched the diagnostic capabilities of deep learning on chest radiographs and an image classifier based on the COVID-Net was presented to classify chest X-Ray images. In the case of a small amount of COVID-19 data, data enhancement was proposed to expanded COVID-19 data 17 times. Our model aims at transfer learning, model integration and classify chest X-Ray images according to three labels: normal, COVID-19 and viral pneumonia. According to the accuracy and loss value, choose the models ResNet-101 and ResNet-152 with good effect for fusion, and dynamically improve their weight ratio during the training process. After training, the model can achieve 96.1% of the types of chest X-Ray images accuracy on the test set. This technology has higher sensitivity than radiologists in the screening and diagnosis of lung nodules. As an auxiliary diagnostic technology, it can help radiologists improve work efficiency and diagnostic accuracy.**

Keywords-deep learning; covid-19 detection; covid-net; transfer learning; model integration

I. INTRODUCTION

The global spread of the COVID-19 pandemic has caused significant losses. The most critical issues, medical and healthcare departments are facing is the fact that the COVID-19 was discovered promptly. Therefore, it is of great importance to check the diagnosis of the suspected case, not only to facilitate the next step for the patients, but also to reduce the number of infected people. X-Ray examination is considered to be the most commonly used X-Ray examination method because of its low cost, wide range of application, and fast speed. It plays a pivotal role in COVID-19 patient screening and disease detection. Because COVID-19 attacks human respiratory epithelial cells, we can use X-Rays to detect the health of the patient's lungs. How to detect these features from X-Ray has become a top priority.

The deep convolutional neural network has achieved unprecedented development in image recognition, especially in the field of auxiliary medical diagnosis technology. Neural networks have been successfully used in identifying pneumonia from X-Rays, achieving performances better than those of radiologists [1].

One of the most significant development is the model COVID-Net proposed by Darwin AI, Canada [2]. A deep convolutional neural network designed to detect COVID-19 cases from chest X-Ray images. At the same time, the chest X-Ray images dataset COVIDx which presented for training and evaluation of COVID-Net was open source.

Ezz El-Din Hemdan et al. proposed the COVIDX-Net based on seven different architectures of DCNNs [3], namely VGG19, DenseNet201 [4], InceptionV2, ResNet101, InceptionV3, Xception and MobileNetV2 [5]. Asmaa Abbas et al. proposed a Decompose, Transfer, and Compose (DeTraC) approach for the classification of COVID-19 chest X-Ray images [6]. This model achieved a sensitivity of 97.91%. Unet based on ResNet50 can also accurately identify the range of double lungs in the chest radiograph and infer the pneumothorax area [7].

This paper aims at the transfer learning and the model combination. Our model is based on COVID-Net which is an open source approach to identify COVID-19. First, load data and solve the problem of data unbalanced. Then combine transfer learning with a modified deep network. Finally, according to the accuracy and loss value, choose the models ResNet-101 and ResNet-152 with good effect for fusion, and dynamically improve their weight ratio during the training process. Form a well closed loop and iteratively update.

II. DATA PREPROCESSING AND TRANSFER LEARNING

A. Loading data to solve unbalanced

In order to verify the feasibility of the method proposed in this paper, a representative data set that was open source during the COVID-19 epidemic was searched. Two data sets were screened out, namely rsna pneumonia dataset and chest X-Ray dataset [8] [9].

Rsna pneumonia detection challenge, which used publicly available cxr data. The training set separated 7966 normal pictures and 8603 other pneumonia pictures. The test set separated 885 normal pictures and 952 other pneumonia pictures.

University of Montreal postdoc Joseph Cohen collected and published a database containing dozens of CT scans and chest X-Ray images. The data set contains 19 cases including Middle East respiratory syndrome, SARS and ARDS. It is still being updated to screen the chest X-Ray images for training purposes. The training set separated 128 COVID-19 pictures and 17 other

This work was supported, the National Natural Science Foundation of China (Grant No. 61871039, 61802019, 61906017), the Supporting Plan for Cultivating High Level Teachers in Colleges and Universities in Beijing (Grant No. IDHT20170511), the Premium Funding Project for Academic Human Resources Development in Beijing Union University (Grant No. BPHR2019AZ01), the Beijing municipal commission of education project (Grant No. KM201911417001), the Big data collaborative innovation center for intelligent driving (Grant No. CYXC1902), Beijing Union University project (202011417004, 202011417005, 202011417SJ025).
* Corresponding author: Hongzhe Liu

pneumonia pictures. The test set separated 12 COVID-19 pictures and 4 other pneumonia pictures. From the data distribution point of view, the number of COVID-19 is very small not only the test set but also the training set.

The distribution of the training set and test set before preprocessing of these two data sets are:

TABLE I. "PREPROCESSING TRAINING DATASET

Dataset	Training Dataset		
	Normal	***Pneumonia***	***COVID-19***
number	7966	8620	128

TABLE II. "PREPROCESSING TESTING DATASET

Dataset	Testing Dataset		
	Normal	***Pneumonia***	***COVID-19***
number	885	956	12

Since it is difficult to distinguish soft tissues with poor contrast in X-Ray images, contrast enhancement is used as a preprocessing step in X-Ray based diagnosis [10].

In addition, as shown in the figure, data enhancement operations such as rotation, sharpening, brightness, and translation are also made a great contribution, which greatly expands the number of COVID-19 data sets. The figure below shows the COVID-19 data set after data enhancement.

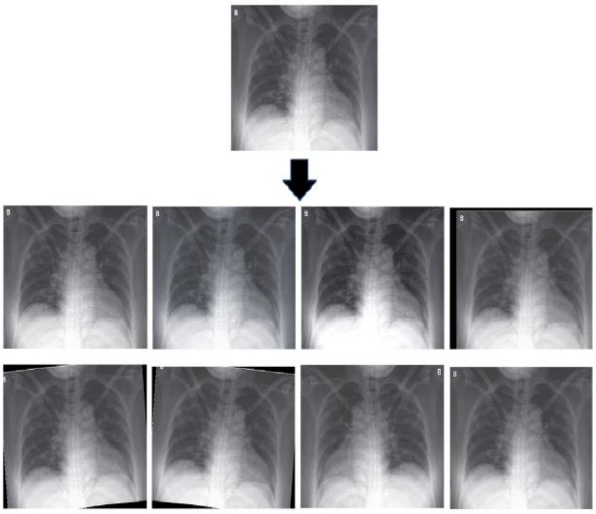

Figure 1. " The effect of data augmentation

B. *Transfer Learning*

The deeper the neural network, the more data training is needed to better fit the parameters of each layer. Otherwise, it is particularly easy to overfit, resulting in a particularly poor generalization ability. In response to this problem, transfer learning provides a feasible solution. It makes full use of the generalization ability of training models on large data sets, and then continues training on smaller chest X-Ray data sets. Doing this, we hope that representations learned by the DNN in the first set can help the model's generalization on the second [11].

ResNet101 and ResNet152 have been trained on the ImageNet dataset [12]. Their generalization performance is particularly great, so the transfer learning can be used as a baseline.

The training process of ResNet101 and ResNet152 transfer learning are similar. Let's take ResNet101 as an example to explain. According to transfer learning, the pre-trained ResNet101 model is used, and the fully connected layer is removed. Then, a new fully connected layer (three labels: normal, COVID-19 and viral pneumonia) consisting of the pooling layer to the softmax was constructed. Finally, a transfer learning model based on ResNet101 is trained. Although the number of training data is very limited, the model does not overfit.

C. *Model Integration*

The two models with the best effect in the transfer learning stage are fused for joint learning. At this stage, we start training by freezing all the network parameters of these two networks. In addition, we give separate weights to the output layers of these two models. The proportion of the output of the two is verified by the test set, and the weight of the higher accuracy rate is higher, and vice versa.

As shown in Fig. 2, the model combination is composed of pretrained model 1 and pretrained model 2. The weight of improving accuracy is improved during the training process. The resulting model is very robust, especially during this training process.

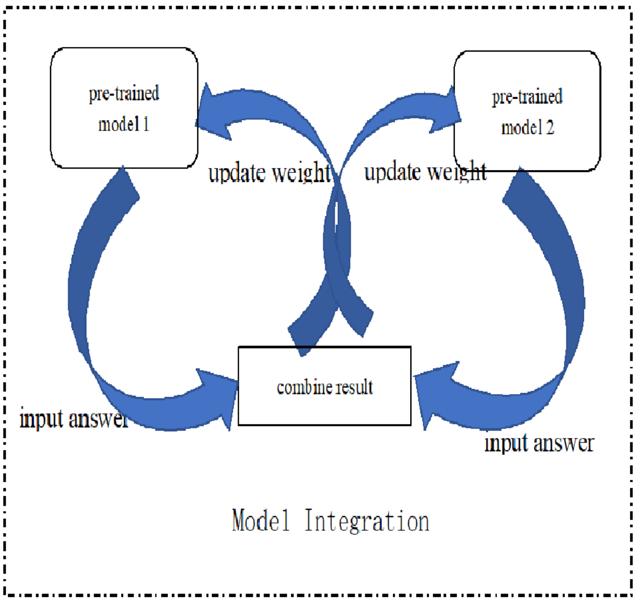

Figure 2. " The structure of model integration

III. EXPERIMENTAL PROCESS AND RESULTS

A. Transfer Learning Training Process

During the training process, in order to make the results reproducible and more convincing, a random seed was fixed. Randomly divide the training set and the test set at a ratio close to 9: 1.

The whole experiment process is shown in Fig.3 which consists of loading image, transfer learning and model combination.

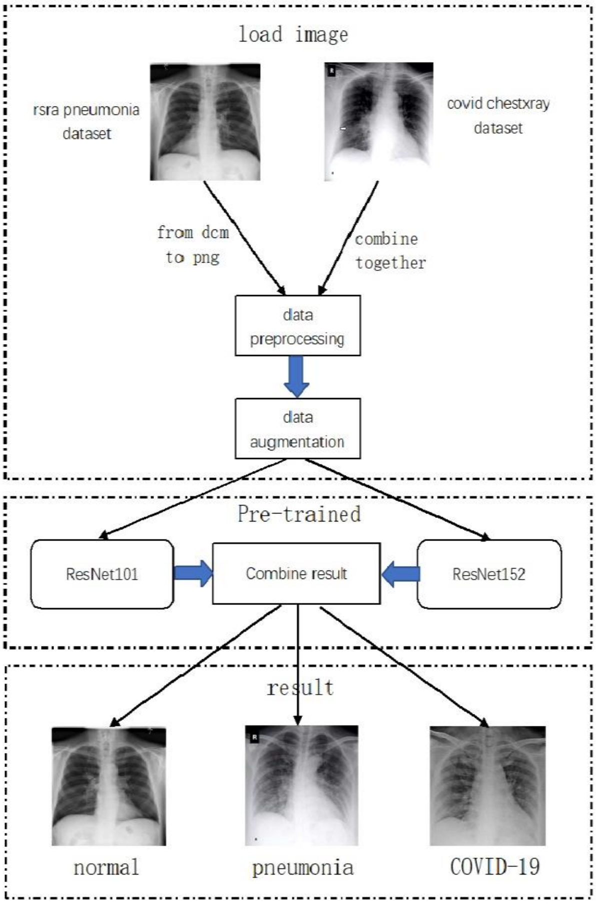

Figure 3. The structure of experiment process

The transfer learning method is adopted, and the trained model is used after transfer learning. We trained on Nvidia GTX 2080 GPU. Before training starts, modify the output layer to adapt the ResNet backbone. Based on transfer learning, in order to make the model converge as soon as possible, set the learning rate to a relatively large value 10^{-4}.

Each batch of 64 pictures, the accuracy and loss value are tested every 50 rounds, the loss and accuracy are displayed in real time through visualization. Tested at the beginning of training, the accuracy rate is bad, and the loss value is also very high. In the first few dozen epochs, the accuracy rate can reach 84.5%, and the situation improves as the training progresses. The accuracy rate has increased significantly, and the downward trend in loss value is also obvious.

Finally, because the model is basically stable, adjust the learning rate to 10^{-5}, that gave us our final network, with a test accuracy of 95.6% and 94.2% respectively. Comparison of the accuracy of several different ResNet skeletons:

TABLE III. ACCURACY OF RESNET SKELETONS

Skeletons	***Accuracy***
ResNet-50	92.4%
ResNet-101	95.6%
ResNet-152	94.2%

B. Model Integration Training Process

The two models with the best effect in the transfer learning stage are fused for joint learning. We start training by freezing these two networks all the network parameters. As the training processes, the accuracy is shown in Fig. 4.

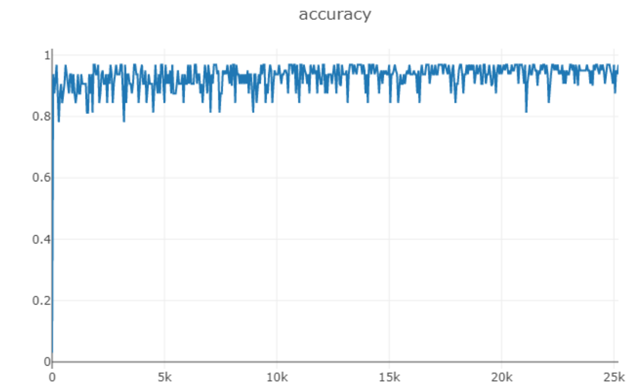

Figure 4. The accuracy of the trainning model

Figure 5. The loss of the trainning model

As shown in the figure above, with the training progresses, the accuracy rate has been very high during the previous verifications. The loss value has not been stable throughout the training process because of the dynamic changes in the weights of the two models. The accuracy of testing a model in the previous round is high, but it is not necessarily the next round, and the weight is improved in the previous round, resulting in slow convergence of loss. After training, the model can achieve 96.1% of the types of chest X-Ray images accuracy on the test set.

IV. CONCLUSION

In response to this outbreak of COVID-19, deep learning has played an indispensable role, which makes it possible to accurately judge and respond to the epidemic. We researched the analytical and diagnostic capabilities of deep learning on chest radiographs and present an image classifier based on the COVID-Net to classify chest X-Ray images. Our model aims at the transfer learning, model integration and classify chest X-Ray images according to three labels: normal, COVID-19 and viral pneumonia. According to the accuracy and loss value, choose the models ResNet-101 and ResNet-152 with good effect for fusion, and dynamically improve their weight ratio during the training process. After training, the model can achieve 96.1% of the types of chest X-Ray images accuracy on the test set.

It provides a reference method for medical and health institutions, government departments and even the global diagnosis of COVID-19 epidemic situation.

REFERENCES

[1] Rajpurkar, P., Irvin, J., Zhu, K., Yang, B., Mehta, H., Duan, T., Ding, D., Bagul, A., Langlotz, C., Shpanskaya, K., Lungren, M.P., Ng, A.Y., 2017. Chexnet: Radiologist-level pneumonia detection on chest x-rays with deep learning. arXiv:1711.05225.

[2] Muhammad Farooq and Abdul Hafeez. Covid-resnet: A deep learning framework for screening of covid19 from radiographs. arXiv preprint arXiv:2003.14395, 2020.

[3] Ezz El-Din Hemdan, Marwa A Shouman, and Mohamed Esmail Karar. Covidx-net: A framework of deep learning classifiers to diagnose covid-19 in x-ray images. arXiv preprint arXiv:2003.11055, 2020.

[4] Xiang Yu, Nianyin Zeng, Shuai Liu, and Yu-Dong Zhang. Utilization of densenet201 for diagnosis of breast abnormality. Machine Vision and Applications, 30(7-8):1135–1144, 2019.

[5] Mark Sandler, Andrew Howard, Menglong Zhu, Andrey Zhmoginov, and Liang-Chieh Chen. Mobilenetv2: Inverted residuals and linear bottlenecks. In Proceedings of the IEEE conference on computer vision and pattern recognition, pages 4510–4520, 2018.

[6] Asmaa Abbas, Mohammed M Abdelsamea, and Mohamed Medhat Gaber. Classification of covid-19 in chest x-ray images using detrac deep convolutional neural network. arXiv preprint arXiv:2003.13815, 2020.

[7] Thomas Brox Olaf Ronneberger, Philipp Fischer. U-net: Convolutional networks for biomedical image segmentation. arXiv:1505.04597 [cs.CV], 2015.

[8] North America, R. S. RSNA pneumonia detection challenge. https://www.kaggle.com/c/rsna-pneumonia-detection-challenge/data (2019).

[9] Cohen, J.P., Morrison, P., Dao, L., 2020. Covid-19 image data collection. arXiv 2003.11597 URL: https://github.com/ieee8023/covid-chestxray-dataset.

[10] Navdeep Kanwal, Akshay Girdhar, and Savita Gupta. Region based adaptive contrast enhancement of medical x-ray images. In 2011 5th International Conference on Bioinformatics and Biomedical Engineering, pages 1–5. IEEE, 2011.

[11] Goodfellow, I., Bengio, Y., Courville, A., Bengio, Y., 2016. Deep learning. volume 1. MIT press Cambridge.

[12] J. Deng, W. Dong, R. Socher, L. Li, Kai Li and Li Fei-Fei, "ImageNet: A large-scale hierarchical image database," 2009 IEEE Conference on Computer Vision and Pattern Recognition, Miami, FL, 2009, pp. 248-255, doi: 10.1109/CVPR.2009.5206848.